



**Impedimetric-based Biosensor for Cardiac Troponin I
Detection: Sensing Strategy aided by Hybrid rGO and
Gold Interdigitated Electrode**

by

**STEVEN A/L TANISELASS
(1741712548)**

A thesis submitted in fulfillment of the requirements for the degree of
Doctor of Philosophy

**Institute of Nano Electronic Engineering
UNIVERSITI MALAYSIA PERLIS**

2021

ACKNOWLEDGMENT

First of all, all praises to Almighty.

I would like to express my sincere thanks to Dato' Prof. Dr. Zul Azhar Zahid Jamal, former Vice Chancellor UniMAP and Prof. Ir. Dr. Rizalafande Che Ismail, former Dean School of Microelectronic Engineering for their support and allowing me to pursue my PhD study. Thank you.

My heartfelt gratitude and a big thanks to my supervisor, Assoc. Prof. Ir. Dr. Mohd Khairuddin Md Arshad for his acceptance and supervision on my PhD. I felt, it's very hard for me to put into words to express my appreciation for your encouragement, guidance, suggestions and supportive nature. Certainly, I have improved my research skill and have learned many things from you during this PhD study. Thank you, Dr. Din. I really wish you will continue your great service to guide and help many students.

My sincere thanks to my co-supervisors, Assoc. Prof. Dr. Subash Gopinath and Dr. Mohd Faris Fathil that have been helped and guided me in my research. Your valuable comments and suggestions are really helped and improved my research work always. Thank you.

Thanks to staff at INEE. Thanks to lab engineers, Mrs. Mira, Mr. Jasni, Mr. Isa, Mr. Luqman, Mr. Bahari Man and Mr. Haffiz Razak. Next, my sincere thanks to all my working colleagues, PhD team-mates; and my FBG friends. All your supports are always there for me. I'm truly appreciate your help and motivations.

Here, I would like to take this opportunity to thank all my teachers that have been thought me since primary school until University-level, without your great guidance I wouldn't be here to write this thesis. Thank you to my all "Guru, Cikgu, Sirs, Teachers and my Lecturers". You are great teachers.

My sincere praises to my parents, parents-in-law, my wife, my son 'Ayden' and my siblings for all your supports and motivations. You are always there for me.

Before I end, once again I take this opportunity to thank entire individual who have been directly or indirectly helped me to complete this thesis. Thanks to all and my apology too for all my mistakes. "*Life is a beautiful journey*".

TABLE OF CONTENTS

	PAGE
DECLARATION OF THESIS	i
TABLE OF CONTENTS	iii
LIST OF TABLES	vii
LIST OF FIGURES	viii
LIST OF ABBREVIATIONS	xiv
LIST OF SYMBOLS	xvii
ABSTRAK	xviii
ABSTRACT	xix
CHAPTER 1 : INTRODUCTION	1
1.1 Background Study	1
1.2 Problem Statements	5
1.3 Research Objectives	7
1.4 Research Scope	7
1.5 Thesis Organization	9
CHAPTER 2 : LITERATURE REVIEW	10
2.1 Introduction	10
2.2 Cardiovascular Diseases	10
2.2.1 Acute Myocardial Infarction	11
2.2.1.1 Cardiac Troponin I Biomarker	12
2.3 Biosensors	14

2.3.1	Electrochemical Biosensors	15
2.3.2	Gold Interdigitated Electrode as Electrochemical Transducer	16
2.3.3	Electrochemical Impedance Spectroscopy	18
2.4	Nanomaterials on Biosensors	20
2.4.1	Graphene-based Nanomaterials	21
2.4.1.1	Pristine Graphene	23
2.4.1.2	Graphene Oxide (GO)	25
2.4.1.3	Reduced Graphene Oxide (rGO)	26
2.5	The Preparations of Graphene-based Nanomaterials	28
2.5.1	The Reduction of GO	29
2.5.2	The Deposition of rGO	33
2.5.3	The Surface Functionalization of rGO	35
2.6	Graphene-based Nanomaterials Characterization Techniques	36
2.7	Graphene-based Electrochemical Biosensors for cTnI Detection	38
2.8	Summary	51
CHAPTER 3 : METHODOLOGY		52
3.1	Introduction	52
3.2	The Preparation of rGO in DIW	54
3.2.1	rGO Dispersion at Various Concentrations and Deposition	54
3.2.2	rGO Suspension Preparation Methods and Single-Droplet Drop-Casting	55
3.2.2.1	Preparation of Microscope Glass Slide	56
3.2.2.2	Preparation of rGO Suspension	57
3.2.2.3	Deposition of rGO Suspension by Drop-Casting	57
3.3	rGO Characterizations	58

3.3.1	Surface Morphological Characterization	58
3.3.2	Structural Characterization	58
3.3.3	Electrical Characterization on Au-IDE	59
3.4	Fabrication of cTnI Immunosensors mediated by rGO	60
3.4.1	Preparation of Au-IDE	61
3.4.2	Surface Modification of Au-IDE	62
3.4.3	Surface Immobilization and Blocking of Au-IDE	65
3.4.4	Sensing Procedure of cTnI in Spiked Buffer	65
3.5	The Sensing Procedure of cTnI in Human Serum	65
3.6	Impedimetric Transduction Procedure	66
3.7	Summary	67
CHAPTER 4 : RESULTS & DISCUSSION		68
4.1	Introduction	68
4.2	Assessments of the rGO Preparations in DIW	69
4.2.1	rGO Nanoflakes Dispersion at Various Concentrations	69
4.2.2	rGO Suspension Preparation Methods and Deposition Analysis	73
4.3	The Characteristics of the rGO Nanoflakes	76
4.3.1	High Power Microscope	77
4.3.2	Scanning Electron Microscope	78
4.3.3	Atomic Force Microscope	79
4.3.4	Ultraviolet Visible Spectroscopy	80
4.3.5	X-ray Diffraction Analysis	81
4.3.6	Raman Spectroscopy	82
4.3.7	X-ray Photoelectron Spectroscopy	84
4.3.8	Fourier Transform Infrared Spectroscopy	85
4.3.9	Electrical Characteristics of the rGO Nanoflakes	86

4.3.9.1	rGO Nanoflakes Deposited on Au-IDE	86
4.3.9.2	Impedance and Reproducibility Assessments	89
4.3.9.3	Current-Voltage (I-V) Characteristics	91
4.4	Assessments of the as-Fabricated cTnI Immunosensors	92
4.4.1	Impedimetric Characteristics of the as-Fabricated Bioelectrodes	93
4.4.2	Impedimetric Characteristics of the cTnI Antigen Detection	95
4.4.3	Validation on Surface Chemistry of Strategy-4	98
4.5	Analytical Characteristics of the cTnI Detection in Human Serum	102
4.5.1	Sample Analysis in Serum and Selectivity	102
4.5.2	Limit of Detection and Sensitivity	105
4.5.3	Reproducibility Test	108
4.5.4	Stability Test	109
4.6	Summary	110
	CHAPTER 5 : CONCLUSION	112
5.1	Introduction	112
5.2	Conclusion	112
5.3	Future Work	115
	REFERENCES	118
	APPENDIX A	142
	LIST OF PUBLICATIONS	147

LIST OF TABLES

		PAGE
Table 2.1	The characteristics of graphene-based nanomaterials - a comparison.	27
Table 2.2	A comparison of electrode surface modifications techniques and the analytical characteristics of label-free cTnI biosensors. The biosensors were developed by using graphene-based nanomaterials and other materials.	50
Table 4.1	Analytical performance comparison of the label-free and rGO based biosensors for cTnI detection.	107

©This item is protected by original copyright

LIST OF FIGURES

	PAGE
Figure 1.1 (a) Schematic illustration of classification and components in biosensor (Y. Zhou et al., 2019). (b) comparison between (i) a label-free and (ii) a label-based immunosensor (Cohen & Walt, 2019).	2
Figure 2.1 The anatomy of heart tissue injury with various possible blood vessel blockage conditions (Thygesen et al., 2018).	12
Figure 2.2 Illustrations represents the structure of cTnI with other biomarkers (Nezami et al., 2018).	13
Figure 2.3 Troponin I concentration level and the related myocardial injury (Fathil & Md Arshad, 2015).	14
Figure 2.4 Basic layout of an electrochemical biosensor (Wongkaew & Simsek, 2019).	16
Figure 2.5 Interdigitated Electrode (IDE). (a) schematic diagram. (b) cross-sectional view. (c) optical image and (d) SEM image (Brosel-Oliu et al., 2019).	17
Figure 2.6 (a) Electrochemical impedance spectroscopy test setup. (b) schematic illustration of Randles equivalent circuit model (Hernández; & Al., 2020) and (c) shows Nyquist plot (Randviir & Banks, 2013).	19
Figure 2.7 Schematic illustration of various nanostructured materials with different dimensions (Qiu, Zhu, & Feng, 2020).	21
Figure 2.8 The primary application of graphene-based nanomaterials in biomedical fields (Qu, He, & Yu, 2018).	23

Figure 2.9	Graphene, GO and rGO synthesis strategies (Tanisclass, Arshad, & Gopinath, 2019).	29
Figure 2.10	The synthesis steps of rGO (Chaudhary, Kumar, Venkatesu, & Masram, 2021).	30
Figure 2.11	Level of green reduction strategies and their related methods (Tanisclass, Md Arshad, & Gopinath, 2019).	33
Figure 2.12	Schematic diagram of electrodeposition and electrophoretic deposition using (a) three-electrode cell and (b) two-electrode cell, respectively (Kurt Urhan & Demir et al., 2020; Ma & Han, 2018).	35
Figure 2.13	Impedimetric curves. (a) surface modification steps (b) cTnI detection at various concentrations (Singal & Srivastava, 2015).	39
Figure 2.14	Detection of cTnI at various concentrations. (a) cyclic voltammetry (b) impedimetric curves (Habib et al., 2016).	41
Figure 2.15	Detection of cTnI at various concentrations. (a) cyclic voltammetry of surface modification steps and (b) linear response of the immunosensor (Z. Li et al., 2017).	42
Figure 2.16	Cyclic voltammetry of cTnI detection at various concentrations ranging from 1 fg - 10 ng/ 6 μ L (Bhatnagar et al., 2017).	43
Figure 2.17	Detection of cTnI. (a) impedance spectra of surface modification steps and (b) differential pulse voltammetry (Sandil et al., 2018).	45
Figure 2.18	Cyclic voltammetry. (a) surface modifications steps and (b) cTnI detection at various concentrations (1 fg - 100 ng/mL) (Chauhan et al., 2020).	47

Figure 2.19	Detection of cTnI. (a) SEM image of the functionalized graphene on IDE and (b) I–V response at various concentrations (Tuteja et al., 2015).	48
Figure 3.1	A flowchart of the research methodology.	53
Figure 3.2	Illustration of three different rGO suspension preparation methods. The methods are denoted as M1, M2 and M3, respectively.	56
Figure 3.3	Schematic illustration of cTnI immunosensor fabrication steps.	61
Figure 3.4	Electrode sensing surface modifications strategies. Strategy-1, Strategy-2, Strategy-3 and Strategy-4 denoted as S-1, S-2, S-3 and S-4, respectively.	64
Figure 4.1	HPM images of the rGO nanoflakes deposited through single-droplet drop-casting onto glass slide. (i) and (ii) at a magnifications of 5X and 50X, respectively.	70
Figure 4.2	HPM images of rGO nanoflakes deposited through single-droplet drop-casting on glass slides. Images (a), (b) and (c) rGO with concentrations of 0.5-, 0.2- and 0.1-mg/mL, respectively. (i) and (ii) at magnifications of 5X and 50X, respectively.	72
Figure 4.3	Digital images. (a), (b) and (c) rGO suspensions from M1, M2 and M3, respectively. Meanwhile (i), (ii) and (iii) the as-deposited rGO from M1, M2 and M3, respectively through single-droplet drop-casting on glass slides.	74
Figure 4.4	HPM images on the single-droplet deposition. (a), (b) and (c) the deposition resulting from M1, M2 and M3, respectively and (i), (ii), (iii) at magnifications of 10X, 20X and 50X, respectively.	76

Figure 4.5	HPM image of the as-deposited rGO nanoflakes at 50X magnification.	77
Figure 4.6	SEM images of the as-deposited rGO nanoflakes. (a) and (b) represent magnifications of 5,000X and 25,000X, respectively.	78
Figure 4.7	AFM images of the rGO nanoflakes. (a) the topographic heights and (b) the 3D image.	79
Figure 4.8	UV-Vis absorption spectra of the rGO nanoflakes, scanned at wavelengths from 200 to 600 nm, with the maximum absorption peak observed at 273 nm and rGO suspension (inset).	81
Figure 4.9	XRD pattern of the rGO nanoflakes, with the 2 theta peak angles appearing at $\sim 23.3^\circ$.	82
Figure 4.10	(a) Raman spectra of the rGO suspension and (b) AFM image of the 2D nanosheets.	83
Figure 4.11	High resolution of deconvoluted Gaussian peaks C1s XPS spectra of rGO nanoflakes.	85
Figure 4.12	FTIR spectra of the rGO nanoflakes.	86
Figure 4.13	Morphological examinations. (a) size comparison between Au-IDE and Malaysian 5 cent coin. (b) HPM image of the bare Au-IDE. (c) HPM image, focus on the deposited rGO nanoflakes on top of Au-IDE surface. (d) SEM image of the as-deposited rGO nanoflakes.	88
Figure 4.14	3D-nano profilometer images. (a) bare Au-IDE and (b) Au-IDE deposited with rGO nanoflakes.	89
Figure 4.15	Electrochemical impedance spectroscopy. (a) bare Au-IDE with inset (i) redox solution resistance and (b) Au-IDE after	

	modification with rGO nanoflakes with inset (i) illustration of rGO modified Au-IDE.	91
Figure 4.16	I-V curves for the rGO/Au-IDE modified sensors with inset shows for bare device.	92
Figure 4.17	Impedimetric curve responses of four surface modifications on respective electrode sensing surface. (a), (b), (c) and (d) impedance measurements for S-1, S-2, S-3 and S-4, respectively exhibits different chemical strategies.	95
Figure 4.18	Impedance curve response of four different chemical strategies. (a), (b), (c) and (d) represent the cTnI detection performance at various target concentrations from S-1, S-2, S-3 and S-4, respectively. (i), (ii), (iii) and (iv) illustrate the predicted chemical bonding for the as-developed bioelectrodes of S-1, S-2, S-3 and S-4, respectively.	97
Figure 4.19	XPS spectral analysis of rGO and rGO + APTES nanohybrid. (a) high resolution of C1s spectra of rGO that was deconvoluted into Gaussian curves. (b) wide energy scan region of XPS of rGO and rGO + APTES nanohybrid.	99
Figure 4.20	XPS spectra of rGO and rGO + APTES nanohybrid of C1s regions.	100
Figure 4.21	FTIR spectra for the rGO and rGO + APTES nanohybrid.	101
Figure 4.22	Impedimetric curve responses (Nyquist plot) of cTnI antigen detection at various concentrations in human serum with (i) inset shows the Randles equivalent circuit.	103
Figure 4.23	Total impedance plotted against a range of frequencies ranging from 0.1 to 500 kHz. Plot from immuno-electrode sensing surface modification steps to cTnI antigen detection at various concentrations.	104

Figure 4.24	Linear regression plot. Mean charge transfer resistance against cTnI antigen detection at various measured concentrations and the estimation of LOD.	106
Figure 4.25	Reproducibility tests. (a) Impedance curve for bare Au-IDE and (b) mean impedance at every electrode surface modification steps, respectively.	109
Figure 4.26	Stability assessment on measurements, tested for a single concentration of cTnI antigen (10 ng/mL).	110
Figure 5.1	An emerging trends in biological recognition elements for AMI diagnosis (Savonnet et al., 2021).	117

©This item is protected by original copyright

LIST OF ABBREVIATIONS

1D	1 Dimensional
2-ABA	2-aminobenzyl Amine
2D	2-Dimensional
3D	3-Dimensional
4-ATP	4-aminothiophenol
AFM	Atomic Force Microscope
Ag	Argentum
AMI	Acute Myocardial Infarction
APTES	(3-Aminopropyl) triethoxysilane
Au	Aurum
Au-IDE	Gold Interdigitated Electrode
Au-SPE	Gold Screen Printed Electrode
BA	Blocking Agent
CK-MB	Creatine Kinase-MB
CNT	Carbon Nanotube
CO ₂	Carbon Dioxide
C-RP	C-reactive Protein
cTnI	Cardiac Troponin I
cTnT	Cardiac Troponin T
CuO	Copper Oxide
CV	Cyclic Voltammetry
CVDs	Cardiovascular Diseases
CVD	Chemical Vapor Deposition
DIW	Deionized Water
DNA	Deoxyribonucleic Acid
DPV	Differential Pulse Voltammetry
EDC	1-ethyl-3-dimethylaminopropyl Carbodiimide
EDX	Energy Dispersive X-ray
EIS	Electrochemical Impedance Spectroscopy
FET	Field-Effect Transistor
FTIR	Fourier-Transform Infrared Spectroscopy
GCE	Glassy Carbon Electrode
GMWCNT	Graphene Multi Walled Carbon Nanotube
GO	Graphene Oxide

GQD	Graphene Quantum Dot
HPM	High Power Microscope
IDE	Interdigitated electrode
ITO	Indium Tin Oxide
LOB	Limit of Blank
LOD	Limit of Detection
M1	Method-1
M2	Method-2
M3	Method-3
Mb	Myoglobin
MnO ₂	Manganese (II) Oxide
NCDs	Noncommunicable Diseases
NHS	N-hydroxysuccinimide
NiO	Nikel Oxide
NMP	N-Methyl-2-Pyrrolidone
PAMAM	Polyamidoamine
PBE	Paper-based Electrode
PBS	Phosphate Buffer Saline
Pd	Palladium
PDDA	Poly-diallyldimethylammonium Chloride
PEI	Polyethyleneimine
Pr-GO	Porous Graphene oxide
Pt	Platinum
rGO	reduced Graphene Oxide
RSD	Relative Standard Deviation
S-1	Strategy-1
S-2	Strategy-2
S-3	Strategy-3
S-4	Strategy-4
SEM	Scanning Electron Microscope
SnO ₂	Tin (II) oxide
SPE	Screen-printed electrode
STM	Scanning Tunneling Microscope
TEM	Transmission Electron Microscope
TiO ₂	Titanium Oxide
UV-Vis	Ultraviolet – Visible

WO ₃ -rGO	Tungsten Trioxide reduced Graphene Oxide
XPS	X-ray Photoelectron Spectroscopy
XRD	X-ray Diffraction
ZnO	Zinc Oxide

©This item is protected by original copyright

LIST OF SYMBOLS

μL	Microliter
μM	Micrometer
\AA	Angstrom
AC	Alternating Current
C	Capacitance
$^{\circ}\text{C}$	Celsius
C_{dl}	Double Layer Capacitance
eV	Electronvolt
G	Conductometric
Hz	Hertz
I	Current
J	Imaginary Part
mM	Milimolar
nM	Nanometer
R	Resistance
R_{ct}	Charge Transfer Resistance
R_{s}	Solution Resistance
V	Voltage
Z	Impedance
Z'	Real-part Impedance
Z''	Imaginary-part Impedance
σ_{lowest}	Standard Deviation of Lowest Concentration
σ_{probe}	Standard Deviation of Probe

Biopenderia berasaskan Permeteran Galangan untuk Pengesanan Troponin Jantung I: Strategik Penderiaan dibantu oleh rGO Hibrid dan Elektrod Berselang-seli Emas

ABSTRAK

Penyakit kardiovaskular (CVD) adalah penyebab nombor satu kematian antara penyakit tidak berjangkit di peringkat global. CVD merujuk kepada penyakit-penyakit yang berkaitan dengan aliran darah yang tidak normal di jantung dan sering dikaitkan dengan keadaan 'serangan jantung' atau dalam istilah klinikal sebagai infarksi miokardium akut (AMI). Biopenanda Troponin jantung I (cTnI) diterima secara meluas sebagai "*piawaian emas*" untuk pengesanan AMI kerana pengkhususannya yang amat tinggi. Oleh itu, keperluan penderia mudah-alih dan peka dengan pengesanan pantas adalah sangat diperlukan untuk mendiagnosis AMI bagi rawatan cepat. Di sini, imunopenderia cTnI berasaskan galangan tanpa-label telah difabrikasi dan prestasi analitik telah dinilai dan dilaporkan dalam tesis ini. Grafena kekurangan oksida (rGO) dan saling berkait elektrod berpadu emas (Au-IDE) digunakan untuk membangunkan imunopenderia. Kaji-selidik ini terbahagi kepada dua bahagian utama; pertama adalah untuk mendapatkan pengendapan rGO yang seragam melalui teknik jatuh-tuangan titisan-tunggal dan yang kedua adalah untuk memfabrikasikan imunopenderia cTnI yang dibantu oleh rGO. Keputusan pengendapan mendedahkan kaedah-3 yang melibatkan teknik pasca-sonikasi menghasilkan nanokepingan rGO yang besar dan memasang-diri melalui jatuh-tuangan titisan-tunggal tanpa menggunakan pelarut kimia. Tambahan pula, peranti Au-IDE yang diubahsuai dengan rGO menunjukkan mobiliti elektron yang sangat baik di mana kekonduksian elektrik meningkat kira-kira 1000 kali ganda berbanding dengan peranti kosong. Oleh itu, ampaiian rGO yang disediakan telah digunakan untuk memfabrikasi imunopenderia. Empat strategik pengubahsuaian permukaan yang berbeza pada bioelektrod masing-masing dibantu oleh ampaiian rGO telah dikaji-selidik. Spektroskopi galangan elektrokimia (EIS) telah dijalankan untuk mencirikan imunopenderia dengan penyapuan frekuensi dari 0.1 - 500 kHz pada voltan AC kecil (25 mV). Hasil kajian menunjukkan bahawa satu daripada empat imunopenderia yang dibangunkan melalui strategik-4 menunjukkan prestasi analitik yang amat baik untuk pengesanan antigen cTnI dalam pepaku penimbal dan serum manusia. Fungsionalisasi permukaan yang berpotensi ini dibantu oleh kumpulan berangkap satah dasar rGO dan telah dipostulat berdasarkan analisa XPS dan FTIR. Imunopenderia yang difabrikasi menunjukkan julat lurus yang luas (10 ag/mL - 100 ng/mL) dalam pengesanan antigen cTnI dalam serum manusia dengan pekali regresi linear (R^2) sebanyak 0.9716 dan analit terendah yang dikesan adalah 10 ag/mL, di mana ia menunjukkan sifat yang sangat selektif dan peka. Imunopenderia ini juga menunjukkan pengesanan pantas yang hanya memerlukan 5 minit untuk kuar dan sasaran mengikat dan stabil selama sembilan hari. Bioelektrod ini boleh dihasilkan semula. Oleh itu, strategik pengubahsuaian permukaan pengesanan elektrod seperti ini dapat diekstrapolasi lebih jauh untuk aplikasi selanjutnya dalam diagnosis berbagai penyakit yang dibantu oleh biopenanda.

Impedimetric-based Biosensor for Cardiac Troponin I Detection: Sensing Strategy aided by Hybrid rGO and Gold Interdigitated Electrode

ABSTRACT

Cardiovascular diseases (CVD) are the number one cause of death among the noncommunicable diseases globally. CVD are referred to diseases that associated with the abnormalities of blood flow in heart and often related with ‘heart attack’ condition or in clinical term as an acute myocardial infarction (AMI). Cardiac Troponin I (cTnI) biomarker is widely accepted as *gold standard* for AMI recognition due to its high specificity. Hence, the need for portable and highly sensitive sensor with fast detection is utmost required to diagnose AMI for fast treatments. Herein, a label-free impedimetric-based cTnI immunosensors were fabricated and their analytical performances were assessed and reported in this thesis. Reduced graphene oxide (rGO) and gold interdigitated electrode (Au-IDE) were employed to develop the immunosensors. The research work is divided into two main sections; first is to obtain a uniform deposition of rGO through single-droplet drop-casting technique and second is to fabricate the cTnI immunosensor aided by rGO. The deposition results revealed the method-3 involving post-sonication technique produces a large and self-assembled of rGO nanoflakes through single-droplet drop-casting without the use of any chemical solvent. Furthermore, the rGO modified Au-IDE devices show an excellent electron mobility, whereby the electrical conductivity was enhanced approximately ~1000-fold compared to the bare devices. Thus, the as-prepared rGO suspension was used to fabricate the immunosensors. Four different surface modification strategies on respective bioelectrodes mediated by the as-prepared rGO suspension were investigated. Electrochemical impedance spectroscopy (EIS) was performed to characterize the immunosensors by sweeping frequencies from 0.1 - 500 kHz at a small AC voltage (25 mV). Results revealed that one of the four immunosensors developed through strategy-4 shows an excellent analytical performance for the cTnI antigen detection in spiked buffer and human serum. A potential surface functionalization mediated by rGO basal plane functional groups was postulated based on XPS and FTIR analyses. The as-fabricated immunosensor showed a wide linear range (10 ag/mL – 100 ng/mL) of cTnI antigen detection in human serum with a linear regression coefficient (R^2) of 0.9716 and the lowest analytes detected was 10 ag/mL, whereby it shows highly selective and sensitive trait. The immunosensor also showed a fast-detection that only required 5 minutes for probe and targets binding and stable for nine days. The bioelectrodes were highly reproducible. Hence, such an electrode sensing surface modifications strategy can be further extrapolated for later applications in various biomarker mediated disease diagnoses.

CHAPTER 1 : INTRODUCTION

1.1 Background Study

Home is a living place for human mankind and biosensors becoming a part of human life which revolutionizing disease diagnosis methods. A biosensor is a diagnostic device predominantly used in healthcare sectors especially for disease recognitions. It offers numerous benefits such as portability, rapid detection, inexpensive, easy to use and eliminates the need for highly trained personnel. Technically, a 'biosensor' is an integrated device that contains two major components namely a biological recognition element (bioreceptor/probe) and a transducer (electrode) where both components are engaged in a specific way to provide a specific analytical information (Ribeiro & Cordeiro, 2020; Sabu & Henna, 2019; Souto, 2017). Figure 1.1 (a) shows the generic components of a biosensor that mainly comprises of bioreceptor and transducer. Biosensors can be classified based on bioreceptors (e.g. DNA biosensors, enzymatic biosensors, immunosensors, aptamer biosensors) or transducers (e.g. optical biosensors, electrochemical biosensors, piezoelectric biosensors). Besides this classification, biosensors also can be categorized as label-based or label-free detection as shown in Figure 1.1 (b). Label-based detection requires "labelling" or "tagging" procedures to bioreceptors in order to detect specific targets (Cohen & Walt, 2019; Sang, Wang, & Feng, 2016). Several examples of label-based detection are fluorescent, chemiluminescent and nanoparticle-labelling. Label-based assay involves more complex procedures, time consuming and requires special instrumentations, thus very expensive (X. Luo, Davis, & Davis, 2013; Syahir & Usui, 2015; Y. Zhou, Fang, & Ramasamy, 2019). Furthermore, some synthetic challenges during labelling procedures may exhibit interference with the

bioreceptor binding site and it could alter an intrinsic nature of the bioreceptor. Meanwhile, a label-free detection has overcome the above-mentioned limitations and it provides a great deal of information on biological interaction event. An electrochemical biosensor is an example of label-free detection. Recently, research on label-free detection by using electrochemical biosensor grows tremendously because it offers numerous benefits such as simple fabrication procedure, real-time diagnosis, high sensitivity, high selectivity and cost effective (Luka & Ahmadi, 2015; Ranjan, Parihar, & Jain, 2020; Roointan, Ahmad Mir, & Ibrahim Wani, 2019). The electrical measurements modes are based on voltammetry, amperometry, conductometric or impedimetric transductions, which depending upon the transducer's structure.

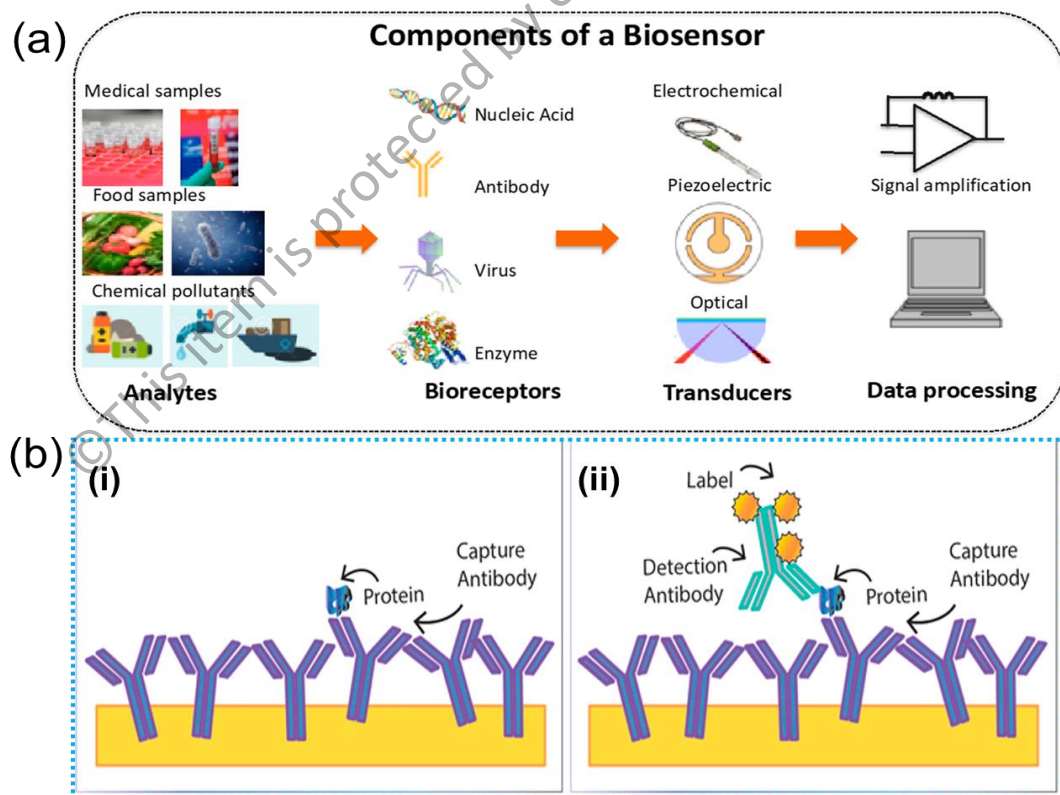


Figure 1.1 (a) Schematic illustration of classification and components in biosensor (Y. Zhou et al., 2019). (b) comparison between (i) a label-free and (ii) a label-based immunosensor (Cohen & Walt, 2019).

In mean time, the advent of nanotechnology has led to application of various types of nanomaterials (carbon-based nanomaterials, metal nanoparticles) in biosensors development. This is due to their high surface area to volume ratio which enhances bioreceptors immobilization area, thus escalates biosensors analytical performance tremendously (eg. limit of detection, sensitivity and selectivity) (W. Jiang, Rutherford, Vuong, & Liu, 2017; Shrivastava et al., 2020). In this context, graphene-based nanomaterials have attracted a strong scientific and technological interest owing to its unique optical, electronic, mechanical, electrochemical and thermal properties (K.S. Novoselov, 2004). The number of research articles that published containing the word “graphene” is significantly increased year by years and the major portion of the research are devoted to biomedical fields, ranging from biosensors, drug delivery, stem cell, tissue engineering and imaging therapy (Mao et al., 2013; Scognamiglio & Arduini, 2019). Graphene was first discovered by A. K Geim and Novoselov through a technique known as mechanical exfoliation or scotch tape cleavage technique (J. W. Jiang, 2015), (Novoselov & Geim, 2004a). Since then, several nanomaterials pertaining to the graphene are known and obtained in the efforts to synthesize the pristine graphene. The nanomaterials can be identified as graphene-based nanomaterials or in other words as ‘graphene derivatives’ which include graphene oxide (GO) and reduced graphene oxide (rGO) (Kochmann, Hirsch, & Wolfbeis, 2012).

Pristine graphene is defined as a single 2D planar/a flat monolayer of sp^2 -bonded carbon atoms that are tightly arranged in honeycombs lattice structure (A. K. Geim, 2007). Graphene having a strong ambipolar electric field effect, a very high crystal quality structure and exhibit massless Dirac fermions characteristics because of the valence band and the conduction band touch the Brillouin zone corners (Mao et al., 2013).

Meanwhile, GO is a precursor material in the effort to synthesis the pristine graphene and it is widely used in micro- and nano-environment especially in biosensors and bioelectronics fields. This is due to a large number of oxygen functional groups in GO (Paredes, Marti, Tasco, & Marti, 2008; Stankovich, Dikin, & Piner, 2007). GO is electrically insulating material because the sp^2 bonding networks are disrupted with oxygen-containing functional groups. The electrical conductivity of GO can be recovered by restoring the π -network through the reduction methods, yielding rGO. In general, rGO is a flat monolayer composed of carbon and oxygen atoms whereby some oxygenated groups have been removed. Hence, the rGO shows an improvement in electrical conductivity and the remaining oxygen groups are still useful to develop biosensors (Gilje, Han, Wang, Wang, & Kaner, 2007). Moreover, rGO also resemble pristine graphene in terms of electrical, thermal, mechanical and optical properties. It exhibits a large surface area to volume ratio with good electrical conductivity that act as “electron wire” between bioreceptor and electrode surface (G. Wei, 2015).

Based on the above literature surveys, clearly a biosensor with label-based detection has its own limitations and the development of label-free biosensor is much preferred. Besides that, an integration of nanomaterials with biosensor hold a great promise for high analytical performances. The nanomaterials can improve biosensor's physicochemical properties such as electro-active surface area and electron transfer rate. The success of the best performs biosensor depend on the right selection of bioreceptors and electrode surface modifications technique (Choudhary, Kumar, & Singh, 2013). Hence, in this thesis, a label-free impedimetric-based biosensor using rGO and gold interdigitated electrode (Au-IDE) is presented to demonstrate the detection of cardiac troponin I (cTnI) biomarker.

1.2 Problem Statements

Cardiovascular diseases (CVD) are the leading cause of death among the noncommunicable diseases (NCDs) globally. According to the latest report based on NCDs country profiles by World Health Organization, the CVD were responsible for 17.9 million death accounting for 44% of total 41 million NCDs death world-widely on 2016 (World Health Organisation, 2018). A CVD is referred to a collection of diseases that associated with abnormalities of blood flow in arteries and is often related to 'heart attack' or in clinical term as an acute myocardial infarction (AMI). It was reported, 85% from 17.9 million of CVD deaths globally was due to heart attack. The current AMI diagnoses methods are based on the analysis from electrocardiogram, echocardiogram, cardiac computer tomographic or coronary angiogram. These methods required hospitalization, medical experts, costly equipment and time-consuming as well as expensive. Hence, an early stage detection plays a vital role in preventing this fatal disease to save human life. With respect to that, cardiac troponin I (cTnI) is considered as *gold standard* biomarker for AMI recognition because it is released from myocardial cells upon cardiac injury and has a very high specificity (Singal & Srivastava, 2014; Tuteja & Bhalla, 2014; Q. Wu, Li, Sun, & Wang, 2017). Thus, a label-free based biosensor with high sensitivity and selectivity that offers fast detection is indeed essential for early treatments. Hence, an integration of rGO with transducer will facilitates to materialise such a high-perform biosensor. However, the development of such biosensor using rGO possess new challenges in the electrode surface modifications. As mentioned earlier, rGO contains plenty amount of oxygen functional groups at the basal plane and at the edge of the nanosheet. The oxygenated groups such as carboxyl and carbonyl are located at the edges, whereas hydroxyl and epoxy are located at the basal plane of the